Pyroxenes from the early and middle stages of fractionation of the Skaergaard intrusion, East Greenland.

(With Plates XVI and XVII.)

By G. M. Brown, M.A., B.Sc., D.Phil., F.G.S.

Department of Geology and Mineralogy, University Museum, Oxford.

With chemical analyses by E. A. Vincent, M.A., B.Sc., Ph.D., F.R.I.C., F.G.S.

Department of Geology and Mineralogy, University Museum, Oxford,

and

P. E. Brown, B.Sc., Ph.D., Department of Geology, University of Manchester.[1]

[Read 28 March 1957.]

Summary. Coexisting calcium-rich and calcium-poor pyroxenes have been separated from the gabbros and ferrogabbros of the Skaergaard layered basic intrusion and chemically analysed. Nine new analyses of augites, three of inverted pigeonites, and one of orthopyroxene are presented, together with optical properties. The trend of crystallization of the augites is different from that drawn by previous investigators. The stages at which the orthopyroxene and pigeonite begin and cease to crystallize are defined, and the sub-solidus exsolution and inversion textures of the pigeonites are examined in detail. The characters of the exsolution textures and the degree of pigeonite inversion (monoclinic to orthorhombic pyroxene) are shown to change gradually with height in the intrusion, and are related to a gradual change in the interval between the temperatures of crystallization and inversion.

SINCE the first description of the trend of crystallization of the Skaergaard clinopyroxenes by Wager and Deer (1939), and the review of the course of crystallization of pyroxenes from mafic magmas by Hess (1941), a great deal of attention has been paid to the character and composition of pyroxenes from basic igneous rocks. Hess plotted the Wo–En–Fs ratio of the chemically analysed pyroxenes of the Stillwater complex and the Skaergaard intrusion and was able to demonstrate a general trend of augite crystallization during the cooling of a mafic magma, and to place the analyses of single pyroxenes from several other igneous bodies on this trend. Up to this stage the trend-line in the ferroaugite region had been tentatively based on only two Skaergaard

[1] Present address: Geological Survey, Tanganyika.

analyses, and more analyses in this region were required. Muir (1951) made fifteen new analyses of clinopyroxenes from the Skaergaard intrusion and drew on a Ca–Mg–Fe diagram (1951, fig. 1) a trend that differed from that of Hess. The marked divergence of the trend in the augite region from that postulated by Hess for pyroxenes from mafic magmas was explained by Muir as due to the unique conditions prevalent at the middle gabbro horizon of the Skaergaard intrusion, where olivines temporarily ceased to crystallize. The trend was drawn in relation to five points believed to be the augite components of five bulk pyroxene analyses; the other component was assumed, in each case, to be a calcium-free hypersthene.

From fresh material collected on the East Greenland Geological Expedition (1953) both calcium-rich and calcium-poor pyroxenes were separated and chemically analysed. The two pyroxenes present in all rocks below, and a few within the ferrogabbro horizon were separated by a magnetic separator and Clerici solution. The trend shown by the augites from this single intrusion does not differ markedly from the composite trend drawn by Hess, and the successive augites and ferro-augites of the Skaergaard intrusion would appear to represent an almost complete series of calcium-rich clinopyroxenes resulting from extreme fractionation of a particular type of basaltic magma.

Hess (1941) clarified pyroxene relationships in slowly cooled mafic magmas by defining the approximate limits of solid solution, the orthopyroxene-pigeonite relationship, and the limit of the field of two-pyroxene crystallization, and by showing the significance of certain exsolution textures. Later Poldervaart and Hess (1951) emphasized the importance of differentiating clearly between the three different groups of pyroxenes crystallizing from basaltic magmas, and summarized the evidence that could be obtained about the cooling history of these magmas from a detailed study of the chemical compositions and textures of the pyroxenes. Muir (1954) and Kuno (1955) have since shown that, under certain physical and chemical conditions, the limits of two-pyroxene crystallization and of solid solution between calcium-rich and calcium-poor pyroxenes, defined by Hess, may not apply.

These papers have directed attention to the value of pyroxenes as a guide to the cooling history of basic magmas. The present investigation was undertaken in order to obtain more detailed information on the two coexisting pyroxene phases from the early and middle stages of fractionation of the Skaergaard intrusion. Further work is in progress on the single pyroxenes from the late fractionation stages, to demonstrate

the behaviour of the pyroxenes throughout extreme fractionation of one type of basic magma.

The pyroxene phases present at different horizons in the intrusion. In

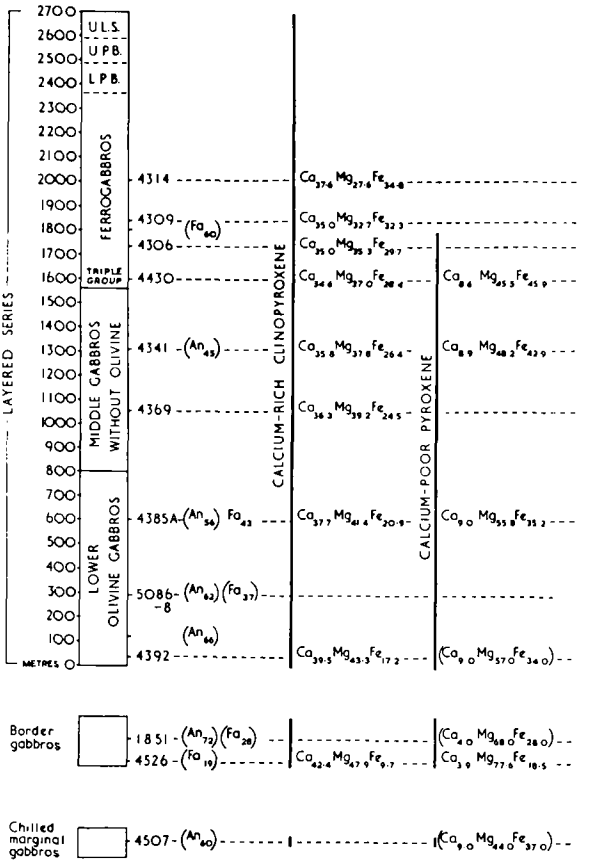

FIG. 1. The relative heights of the rocks of the Skaergaard intrusion from which pyroxenes have been analysed. Compositions of other minerals, if obtained from optical properties, are in brackets.

the chilled marginal gabbro, representing the quickly cooled initial liquid, both augite and pigeonite (subsequently inverted to orthorhombic pyroxene) have crystallized (fig. 1). Rocks formed of the earliest crystal fractions from the slow cooling of this liquid are found next to the chilled margin in the outer part of the narrow marginal border group.

A much greater thickness of similar rocks, forming part of the layered series, is believed to lie hidden below the present level of erosion. The process of formation of the marginal border group is more difficult to understand than is that of the layered series, but three important rock types were recognized by Wager and Deer (1939, p. 137): the gabbro-picrite, rich in a magnesian olivine (Fa_{19}); the perpendicular-felspar rock, rich in a basic plagioclase felspar (An_{70}); and the wavy-pyroxene rock, rich in an iron-poor augite.

The gabbro-picrite contains a diopsidic augite in small euhedral crystals together with orthopyroxene as poikilitic plates. Orthopyroxene is only found in the gabbro-picrite and the perpendicular-felspar rock, although it is reasonable to suggest that it may occur in the lower rocks of the hidden layered series. In the wavy-pyroxene rock, which occurs in a zone farther from the margin than that containing the gabbro-picrite and perpendicular-felspar rock, the calcium-poor pyroxene phase is an inverted pigeonite rather than orthopyroxene. Thus in the earliest stages of crystallization through fractionation of the Skaergaard magma, a clinopyroxene and an orthorhombic pyroxene were the pyroxene phases to crystallize in equilibrium, but the calcium-poor pyroxene later became a pigeonite rather than an orthopyroxene.

The lowest exposed rocks of the layered series contain augite and a hypersthene formed from inversion of pigeonite (see p. 529 for proof), so the name 'lower olivine gabbro' is used in this paper, in preference to the earlier-used name of 'hypersthene olivine gabbro'. From 0 to 250 m., only the olivine and felspar occur as a primary precipitate, and the pyroxenes appear to have crystallized entirely from the inter-precipitate liquid. However, this evidence does not entirely preclude their crystallization as a primary precipitate in the hidden layered rocks. Above the 250-m. level augite is certainly a primary precipitate mineral, and a little later pigeonite (now inverted) apparently became a primary precipitate phase and together with the olivine and felspar may be concentrated in thin layers.

From 800 m. to 1550 m. (the middle gabbros) olivine fails to crystallize as a primary precipitate. The absence of olivine has apparently no effect on the character of the pyroxenes, a primary precipitate augite crystallizing in equilibrium with a primary precipitate pigeonite (usually inverted) to the 1800-m. level. Towards the top of the middle gabbros and in the lower part of the ferrogabbros (1300-m. to 1800-m. level) a few of the rocks contain grains of uninverted pigeonite. The proportion of uninverted to inverted pigeonite is rarely greater than about 10 %, the highest

value being reached in the upper levels, just before the pigeonite phase disappears.

At approximately the 1800-m. level pigeonite ceased to crystallize and a ferroaugite is the only pyroxene phase present in the increasingly iron-rich ferrogabbros and later rocks. The behaviour of the ferroaugites towards the top of the intrusion has been described by Wager and Deer (1939) and Muir (1951), and further work in progress on these pyroxenes, by L. R. Wager and others, will be described in a later paper.

Chemical analysis of selected pyroxenes. The chemical analyses by E. A. V. (see key to table I) were made on a semi-micro scale; all main portions on samples of less than $\frac{1}{2}$ g., and nine of the twelve on samples of less than 150 mg. (the smallest sample analysed was no. 7, of 41 mg.). With this advantage it was possible to work on small fractions, usually of pure material; it would have been impracticable to separate the large amounts required for macro-analysis, of comparable purity, from the middle gabbros and lower ferrogabbros (fig. 1) where augites and pigeonites are closely intergrown.

The analyses (table I) have been recalculated into the standard formula $(WXY)_2Z_2O_6$ (table II), in order to demonstrate both the balance of charge and the variation in cation proportions throughout the fractionation sequence represented by analyses 1 to 10. In order to calculate the distribution of the cations between the (WXY) group (8-fold and 6-fold coordination) and the (Z) group (4-fold coordination), the method described by Hess (1949, p. 625) is believed to be of most value. Thus instead of making $Z = 2$ by adding arbitrary amounts of Al, and occasionally Ti and Fe''', to the Si (e.g. Kuno, 1955, p. 85), the cations are allotted to groups in accordance with the balance of charge on a cation for cation basis (e.g. $NaFe''':Si$; $Fe''':Al$; and $Al:Al$). By this method it is possible to estimate the proportion of Al, Ti^{IV}, and Fe''' likely to be replacing Si in the tetrahedral sites, and their effect, in this position, on the optical properties and unit-cell dimensions.

The variation in the principal cations Ca, Mg, and Fe'' during fractionation is best seen by reference to fig. 2 and is discussed in the following section. However, several of the other cations show a regular pattern in their distribution, which can be seen in table II. The Al in augites and in calcium-poor pyroxenes decreases steadily during fractionation, both in the (Z) and in the (WXY) groups, the decrease being more marked and regular for the augites. The augite always contains more Al in the (Z) group than does the calcium-poor pyroxene from the same rock, but contains about the same (perhaps slightly less) in the (WXY) group.

TABLE I. Analyses and optical properties of the pyroxenes. (All refractive indices $\pm 0{\cdot}001$; $2V \pm 1°$. Data are for the host orthopyroxene in analyses 4A, 6A, and 7A. For the key to these analyses see p. 518.)

	1.	1A.	3.	4.	4A.	5.	6.	6A.	7.	7A.	8.	9.	10.
SiO_2	51·17	53·6	51·25	50·66	50·35	51·26	51·26	50·9	50·58	50·5	50·33	50·10	49·73
Al_2O_3	3·22	2·3	2·92	2·45	2·23	2·23	1·98	1·8	2·20	1·3	2·12	1·30	1·39
Fe_2O_3	1·53	1·3	1·70	1·33	1·14	1·25	1·25	0·7	1·57	0·7	1·69	1·51	1·50
FeO	4·54	10·8	8·87	11·24	21·12	13·34	14·49	25·1	15·53	27·0	16·32	17·89	19·28
MnO	0·13	0·3	0·18	0·29	0·38	0·34	0·35	0·3	0·28	0·2	0·23	0·43	0·41
MgO	16·68	28·7	15·04	14·25	20·03	13·40	12·85	16·4	12·60	15·5	11·92	11·17	9·40
CaO	20·54	2·0	19·04	18·01	4·50	17·23	16·91	4·2	16·40	4·1	16·48	16·68	17·75
Na_2O	0·65	0·2	0·37	0·36	—	0·26	0·26	0·1	0·24	0·2	0·25	0·25	0·24
K_2O	0·05	$0{\cdot}0_3$	0·05	0·08	—	0·02	0·02	$0{\cdot}0_4$	0·03	0·1	0·03	0·02	0·02
TiO_2	0·97	0·5	0·76	1·30	0·55	0·80	0·84	0·5	0·61	0·4	0·71	1·31	0·77
Cr_2O_3	0·42	0·3	0·17	n.d.*	n.d.	< 0·01	< 0·01	n.d.	< 0·01	n.d.	n.d.	n.d.	n.d.
	99·90	$100{\cdot}0_3$	100·35	99·97	100·30	100·13	100·21	$100{\cdot}0_4$	100·04	100·0	100·08	100·66	100·49
β	1·691	—	1·695	1·697	—	1·700(5)	1·702	—	1·704	—	1·707	1·710	1·714
γ	—	1·689	—	—	1·714	—	—	1·723	—	1·727	—	—	—
2V	47°(+)	75°(−)	45°(+)	42°(+)	53°(−)	41°(+)	41°(+) to 44°(+)	47°(−)	40°(+) to 42°(+)	46°(−)	40°(+)	42°(+)	46½°(+)
Exsolution lamellae	None	(100)	(100) and (001)	(001)	complex	(001)	(001)	complex	(001)	complex	(001)	(001)	None
Atomic %													
Ca	42·4	3·9	39·5	37·7	9·0	36·3	35·8	8·9	34·6	8·6	35·0	35·0	37·6
Mg	47·9	77·6	43·3	41·4	55·8	39·2	37·8	48·2	37·0	45·5	35·3	32·7	27·6
Fe	9·7	18·5	17·2	20·9	35·2	24·5	26·4	42·9	28·4	45·9	29·7	32·3	34·8

* $Cr_2O_3 = 0{\cdot}06$ % in augite of 4389, of similar horizon and almost identical composition to 4385A (analyst, E. A. V.).

TABLE II. Formulae of the analysed pyroxenes (on the basis of six oxygen atoms) arranged in their order of crystallization during fractionation. (Note the changes in the amount of each cation during fractionation, and also the relative distribution of minor cations between the calcium-poor pyroxenes 1A, 4A, 6A, 7A and the corresponding calcium-rich pyroxenes 1, 4, 6, 7.)

		1.	1A.	3.	4.	4A.	5.	6.	6A.	7.	7A.	8.	9.	10.
Z	Si	1·882	1·911	1·904	1·903	1·895	1·932	1·937	1·947	1·925	1·952	1·923	1·924	1·931
	Al	0·099	0·074	0·097	0·094	0·081	0·081	0·078	0·059	0·080	0·042	0·081	0·060	0·063
	Ti	—	—	—	—	—	—	—	—	—	—	—	0·020	0·005
WXY	Al	0·040	0·023	0·030	0·015	0·018	0·018	0·010	0·022	0·018	0·019	0·013	—	—
	Fe‴	0·042	0·034	0·047	0·038	0·032	0·036	0·036	0·021	0·046	0·021	0·048	0·044	0·044
	Fe″	0·139	0·321	0·277	0·354	0·665	0·421	0·458	0·801	0·494	0·873	0·521	0·574	0·625
	Mn	0·004	0·009	0·007	0·009	0·011	0·011	0·011	0·011	0·009	0·007	0·007	0·014	0·014
	Mg	0·915	1·526	0·833	0·797	1·124	0·751	0·724	0·935	0·716	0·891	0·684	0·639	0·543
	Ca	0·809	0·077	0·759	0·725	0·181	0·695	0·685	0·172	0·668	0·169	0·675	0·685	0·739
	Na	0·046	0·015	0·027	0·027	n.d.	0·018	0·018	0·009	0·018	0·014	0·018	0·018	0·019
	K	0·002	0·002	0·002	0·004	n.d.	—	—	0·002	0·002	0·004	0·002	—	—
	Ti	0·027	0·013	0·022	0·036	0·016	0·023	0·025	0·014	0·018	0·012	0·021	0·017	0·019
	Cr	0·013	0·009	0·004	n.d.*	n.d.	—	—	n.d.	—	n.d.	n.d.	n.d.	n.d.
Z		1·981	1·985	2·001	1·997	1·976	2·013	2·015	2·006	2·005	1·994	2·004	2·004	1·999
WXY		2·037	2·029	2·008	2·005	2·047	1·973	1·967	1·987	1·989	2·010	1·989	1·991	2·003
% Al in Z		5·0	3·7	4·8	4·7	4·1	4·0	3·9	2·9	4·0	2·1	4·0	3·0	3·2
% Ti in Z		—	—	—	—	—	—	—	—	—	—	—	1·0	0·3

* Cr = 0·002 in augite of 4389, of similar horizon and almost identical composition to 4385A.

KEY TO TABLES I AND II.

1 Augite from gabbro-picrite, 4526.
1A Bronzite from gabbro-picrite, 4526. Analysis obtained by subtracting 5·2 % of analysed augite (1) from analysis of contaminated sample and recalculating to 100 %.
3 Augite from lower olivine gabbro, 4392.
4 Augite from lower olivine gabbro, 4385A.
4A Pigeonite from lower olivine gabbro, 4385A.
5 Augite from middle gabbro, 4369.
6 Augite from middle gabbro, 4341.
6A Pigeonite from middle gabbro, 4341. Analysis obtained by subtracting 3·8 % of analysed augite (6) from analysis of contaminated sample and recalculating to 100 %.
7 Augite from ferrogabbro, 4430.
7A Pigeonite from ferrogabbro, 4430. Analysis obtained by subtracting 10 % of analysed augite (7) from analysis of contaminated sample and recalculating to 100 %.
8 Augite from ferrogabbro, 4306.
9 Augite from ferrogabbro, 4309.
10 Augite from ferrogabbro, 4314.

See fig. 1 for height of the rocks in a vertical succession.

Analyses 1, 1A, 3, 5, 6, 6A, 7, 7A, 8, 9, 10 by E. A. Vincent.

Analyses and separation of 4, 4A by P. E. Brown.

A few augites are slightly zoned with an irregular narrow outer rim having 2V up to 3° greater than that of the main part of the crystal. Although too sporadically developed to take into account, this will have some effect on the accuracy of a correlation between optical properties and chemical compositions.

The Na and Cr contents decrease during fractionation, the Fe‴ remains remarkably constant, while the Mn shows a very slight overall increase in the later stages. The K remains very low throughout the series. The Ti content hardly varies, except that in specimens 9 and 10 the charge balance requires a small amount of Ti in the (*Z*) group. This unusual condition is not related to a progressive increase during fractionation because later pyroxenes in the sequence (to be published later) contain amounts comparable with those of specimens 1 to 8. Despite the unusual distribution of Ti in these two augites the TiO_2 % is not abnormally high (cf. Wilkinson 1956, table II, in which the high TiO_2 % of 56 clinopyroxenes from alkali olivine-basalt magmas is demonstrated). The entry of Ti into the (*Z*) group is also a function of Al_2O_3 content, and pyroxenes with a higher TiO_2 content than these Skaergaard augites may not contain Ti in the (*Z*) group, provided the Al_2O_3 content is high enough (e.g. Hess, 1949, analyses 24 to 26).

When the compositions of coexisting augites and calcium-poor pyroxenes are considered it is seen that the augites are, in each case, relatively enriched in Al (*Z* group), Fe‴, Na, Ti, and Cr.

The nature of the gradual changes in character and composition of the

Skaergaard pyroxenes during fractionation. The pyroxenes that crystallized from the Skaergaard magma changed gradually in character and composition (related to Ca:Mg:Fe ratio) over a considerable range during fractionation (fig. 1). The changes resemble those summarized by Poldervaart and Hess (1951), who predicted the range and sequence of changes for pyroxenes from a single body of strongly fractionated

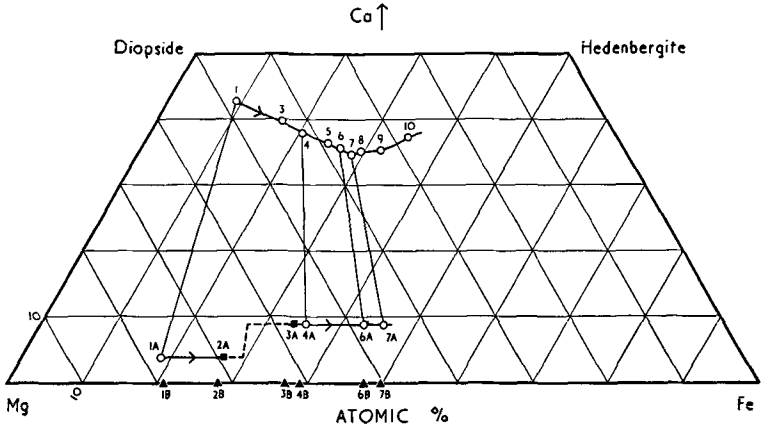

FIG. 2. Trend of crystallization of calcium-rich and calcium-poor Skaergaard pyroxenes; ○ analysed specimens (1 to 10, augite; 1A, orthopyroxene; 4A to 7A, pigeonite); ▲ composition, as Fe:Mg ratio, derived from optical properties (1F, 2B, primary orthopyroxene; 3B to 7B, orthopyroxene from pigeonite inversion); ■ composition, as Ca:Mg:Fe ratio, derived from optical properties and the assumption of standard calcium content in orthopyroxene and pigeonite.

basaltic magma by assembling evidence, at several fractionation stages, from different intrusions.

The textures of the earliest crystal accumulate, the gabbro-picrite, indicate that although olivine probably began to crystallize before pyroxene, it was soon joined by a diopsidic clinopyroxene (no. 1, fig. 2), while poikilitic plates of orthopyroxene (no. 1A, fig. 2) grew from the interprecipitate liquid. The presence of orthopyroxene rather than pigeonite at this stage indicates crystallization of the calcium-poor phase below the clinopyroxene–orthopyroxene inversion temperature curve (cf. Hess, 1941, fig. 9), while the presence of inverted pigeonite in the chilled margin indicates crystallization of this pyroxene phase above the inversion curve, the subsequent inversion to orthopyroxene taking place at sub-solidus temperatures.

In order to represent this relationship a diagram including both solidus

and liquidus curves, in addition to the inversion curve, is necessary (fig. 5; construction explained in Appendix, p. 541). The gabbro-picrite contains orthopyroxene (*B*) as the calcium-poor phase, while the chilled magma (EG 4507) contains pigeonite (*D*), now inverted. If the magma at the commencement of pyroxene crystallization is represented by

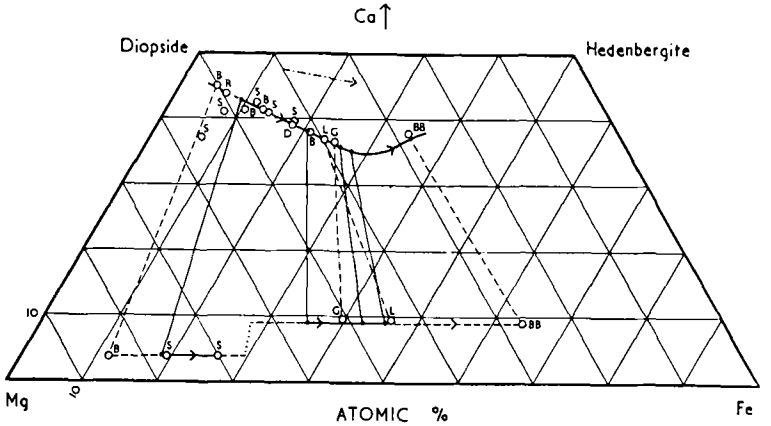

FIG. 3. Pyroxenes from well-described, slowly cooled, tholeiitic-basalt magmas plotted in relation to the Skaergaard trends. Apart from two augites from the Stillwater complex the plot indicates a well-defined general trend of crystallization, both for calcium-rich and calcium-poor pyroxenes. The tie-lines between analysed pairs of pyroxenes from the same rock are shown. —— ·—— Skaergaard intrusion (· analysed co-existing pairs); – – – other intrusions; · · · · · probable inversion interval for plutonic pyroxenes (cf. Kuno and Nagashima, 1952, p. 1001, for volcanic pyroxenes); – · – · → general trend of augites from alkali-basalt magmas (Wilkinson, 1956). B = Bushveld, D = Duluth, G = Goose Creek, L = Lambertville, S = Stillwater (Hess, 1949 and 1952); BB = Beaver Bay (Muir, 1954); R = Rhum (Brown, 1956).

point *C* in fig. 5, chilling with supercooling of the liquid will result in the crystallization of pigeonite at point *D*. Further cooling will result in inversion to orthopyroxene. With slow cooling of this magma, on the other hand, pyroxenes (*B*) representing the solid phase in equilibrium with liquid *C* at this temperature will separate, and in view of their composition will crystallize as orthorhombic pyroxene. Pyroxenes *B* and *D* bear a relationship similar to that of intratelluric pyroxene phenocrysts to groundmass pyroxenes of a porphyritic lava (*P*1, *G*1, ..., fig. 5).

The perpendicular-felspar rock, which crystallized as part of the marginal border group, but later than the gabbro-picrite, also contains

augite and orthopyroxene, the latter (no. 2A, fig. 2) lying between *B* and *P*1 (fig. 5) in composition. The last important rock type to crystallize in the marginal border group is the wavy-pyroxene rock, which contains rare inverted pigeonite of composition close to that of *D* (fig. 5).

The lower olivine gabbros, of which 4392 (fig. 1) is an example, contain both augite (no. 3, fig. 2) and rare inverted pigeonite, in each case as poikilitic plates enwrapping olivine and plagioclase. Easily recognizable primary precipitate crystals of augite and pigeonite are not found until 250 m. above the base of the exposed layered series, and it is not easy to predict the character of the pyroxenes in the hidden layered series. By analogy with other intrusions (e.g. Hess, 1949) it might be expected that after the deposition of the gabbro-picrite a series of clinopyroxenes would crystallize between augites 1 and 3 (fig. 2), in equilibrium at first with orthopyroxenes (such as 2A) and later with pigeonites. The hidden layered series, in all probability, contains the clue as to the position at which a pigeonite, rather than an orthopyroxene, begins to crystallize in equilibrium with augite. In view of the lack of evidence for this position in the Skaergaard intrusion, the transition from orthopyroxene to pigeonite has been placed (fig. 2) at the stage defined by Kuno and Nagashima (1952, fig. 2).

For the first 250 m. of the lower olivine gabbros it is not uncommon to see orthopyroxene free from coarse exsolution lamellae forming narrow extensions to the variety rich in blebs and lamellae, thought to be inverted pigeonite. As the trend of fractionation is from orthopyroxene to pigeonite this relationship is unexpected. If the observed relationship were due to growth of the orthopyroxenes from the late residual liquid after the temperature had dropped below the inversion temperature, the composition of the orthopyroxene ought to be more ferriferous than the host orthopyroxene of the inverted pigeonite. In fact the two are identical in composition, and the relationship may possibly be explained by assuming that the whole grain (core plus extension) was originally pigeonite, and that exsolution began at the centre, the exsolved material from the rim migrating there and leaving the extension free from exsolution lamellae. The texture shown in pl. XVII, fig. 7, would be difficult to explain on any other hypothesis.

At the 600-m. level augite and pigeonite co-exist as a primary precipitate, and both have been analysed from 4385A (fig. 2, nos. 4 and 4A). The pyroxenes throughout the lower olivine gabbros vary little in composition, considering the thickness of gabbro involved. By comparing the change in composition of pyroxenes 1 to 3 with that of pyroxenes 3

to 5, then, assuming a similar rate of fractionation, some estimate of the great thickness of hidden layered series can be obtained.

At 800 m. olivine ceased to crystallize, and the olivine-free middle gabbro series begins. Two typical rocks of this group, 4369 and 4341, still contain augite and pigeonite as a primary precipitate, and the four minerals have been analysed. The analyses show that the disappearance of olivine does not produce a sharp change in the trend-line (fig. 2), as suggested by Muir (1951, fig. 1). The rate of fractionation, as illustrated by the change in pyroxene composition with height in the intrusion, is seen to be increasing markedly. The habits of the augite and pigeonite have changed slowly through the lower olivine gabbro and the middle gabbro horizons. In rocks such as 4369 the discrete, primary-precipitate character of the pigeonite is more easy to detect than at lower horizons, possibly owing to there being less material added to these grains, in the form of irregular extensions, from the interprecipitate liquid. The pigeonite and augite tend to occur together in aggregates of four to six grains. In 4341 and higher in the succession these aggregates of pyroxene grains have become the most distinctive textural feature, the pigeonites being even more uniform in size and shape than in 4369 (fig. 4). The clusters of pyroxenes usually consist of at least twelve (often twenty) grains of augite and pigeonite. Though closely packed they are rarely intergrown. A few of the grains of pigeonite, in 4341, show only partial inversion to orthopyroxene.

Olivine is found as a primary precipitate in 4429 (1570 m.) and after 770 m. of middle gabbros this marks the beginning of the ferro-gabbros in the layered series. From 20 m. above this horizon ferrogabbro 4430 was collected and found to contain, as well as olivine, augite and pigeonite with the same habit and proportions as in 4341, except that the close packing of the two pyroxenes has become even more impressive. In the rocks from this horizon the contact between adjacent augites and the pigeonites is frequently marked by intergrowth. The large patches of pyroxene are only resolved into their component grains under crossed nicols, the texture being reminiscent of that found in the pyroxenes low in the purple band and attributed by Wager and Deer (1939, p. 111) to the inversion of wollastonite. Although the augites are mainly pale brown at these horizons in the large clusters they are pale-coloured where, at the centres of the clusters, several are in contact. The pale-coloured part of each grain has a 2V which is 5° to 7° higher than the brown part, while associated with it are a few discrete grains of orthopyroxene, hornblende, and chlorite. It looks as though, with lowering temperatures

and increasing volatiles in the interstitial liquid between the grains of each cluster, the orthopyroxene component was completely exsolved from the augites, leaving the latter more calcic. The two pyroxenes from 4430 (brown augite and pigeonite) were separated with difficulty and analysed; the results show no marked change in direction of the trend-line of the augites and ferroaugites with the renewed precipitation of

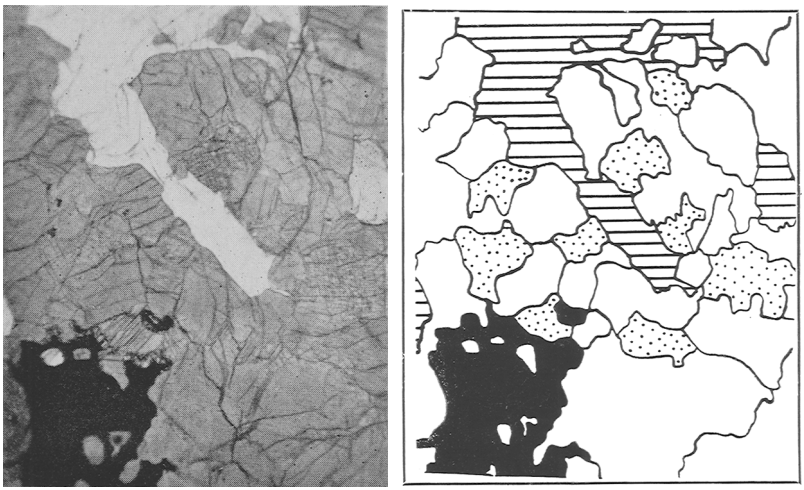

FIG. 4A (left). Photomicrograph of middle gabbro (4341) showing typical closely-packed aggregate of discrete crystals of augite and inverted pigeonite, found to be increasingly common as the limit of two-pyroxene crystallization is approached. Ordinary light. × 18.

FIG. 4B (right). Tracing of fig. 4A to distinguish between pigeonite (stippled) and augite (clear), and between individual crystals of augite (olivine reaction rims are, together with iron ore, black).

olivine as a primary phase. A suitably orientated grain of uninverted pigeonite from 4432 (30 m. above 4430) had $2V+16°$.

One or two small grains of pigeonite were seen in thin sections of 4306 to 4309, 150 m. above 4430, but it was impossible to separate them for analysis. This horizon (1740 to 1840 m.) has therefore been designated the highest at which two pyroxenes are found, although the analysis of the pigeonite from 4430 (150 m. below) is the closest available estimate of the composition of the last calcium-poor pyroxene to crystallize. From simple extrapolation it is unlikely, however, that the Fe content (as a percentage of Ca+Mg+Fe) of the last pigeonite will exceed Fe_{55}.

It is not practicable to state the horizon at which the limit of the two-pyroxene field[1] is reached more precisely, because it is not clear whether the odd grains of pigeonite in rocks 4306 to 4309 were crystallizing in equilibrium with augite, or were held in suspension rather longer than the last main batch.

The cessation of pigeonite crystallization, somewhere between 4306 and 4309 (analyses 8 and 9, fig. 2), implies a passage of the magma from the field of two-pyroxene to that of one-pyroxene crystallization. The compositions of these two augites, which fall on each side of the field limit, prove that there is no marked compositional break at the limit, but a gradual change in the direction of the fractionation trend towards calcium enrichment. Of particular significance is the fact that the disappearance of the calcium-poor pyroxene phase is not accompanied by the crystallization of a single pyroxene with calcium content intermediate between the calcium-rich and calcium-poor phases. The augites and ferroaugites from 4306 and 4309 (1740 to 1840 m.) each contain 35 % Ca of total Ca+Mg+Fe and illustrate clearly that for the Skaergaard series this is the maximum replacement of the larger Ca by the smaller Mg and Fe ions.

Augites from 4309 and 4314 (nos. 9 and 10, fig. 2) are almost uniform in character, being deep brown in colour and almost free from exsolution lamellae, apart from the schiller-structure (p. 528) noted in the augites from rocks 4306 to 4310. The only exception to the uniformity is the presence of fingers of pale-coloured augite intergrown with the brown augite in narrow zones at the contact with iron ores. The pale augite is optically discontinuous with the brown variety, and has a 2V 6° to 10° greater than the latter. The textures suggest that it has formed by reaction between interstitial liquid and iron ore (the iron-rich varieties having higher optic angles in this range), but it is surprising that the reaction product has not grown as an optically continuous zone to the brown augite, but is intergrown in a fashion that suggests a structural break between the two varieties.

The limit of the two-pyroxene field. Three hypotheses have been advanced by previous investigators to explain why, in the later stages of fractionation of a basaltic magma, the calcium-poor pyroxene ceases to crystallize. There may be reaction of the calcium-poor pyroxene with the liquid to form a fayalitic olivine (Poldervaart and Hess, 1951, p. 479);

[1] The term 'two-pyroxene boundary' was used by Hess (1941) to define this limit, but by Tsuboi (1932) to define the binary cotectic. The term 'limit of the two-pyroxene field' is used in this account to avoid this ambiguity.

the binary cotectic relationship between calcium-rich and calcium-poor pyroxene may at this boundary cease to exist, being replaced by a solid-solution with a minimum (Hess, 1941, and Tsuboi, 1932); or the minimum of the liquidus may migrate towards one of the limbs of the solvus until it passes beyond the limit of intersection with the solvus, when either a lime-rich or a lime-poor pyroxene will crystallize (Muir, 1954, p. 384 and fig. 4).

Both augites and pigeonites have now been analysed from the horizons in the Skaergaard intrusion just before, during, and after the stage at which olivine failed to crystallize as a primary precipitate phase. It is now clear that at these stages there was no marked change in the composition of the pyroxenes, and it can be assumed that there is no simple, sympathetic relationship between the crystallization of olivine and of calcium-poor pyroxene.

If, during iron enrichment, the slope of the crest of the solvus exceeds the slope of the liquidus minimum, then a temperature might be reached when the solidus of the solid-solution series no longer intersects the solvus and one pyroxene would crystallize instead of two. In order to apply this hypothesis it is necessary to know the slopes of both the liquidus minimum and the crest of the solvus from the diopside-clinoenstatite boundary to the hedenbergite-ferrosilite boundary, and even then the effect of other constituents, particularly volatiles, in the magma would have to be considered. The experimental work of Bowen (1914) and of Bowen, Schairer, and Posnjak (1933) has provided an estimate of the slope of the solid-solution minimum, from about 1400° C. for diopside-clinoenstatite to about 950° C. for hedenbergite-ferrosilite. The crest of the solvus for diopside-clinoenstatite has been shown to be at 1380° C. by Atlas (1952, fig. 4), but nothing is known of the temperature of the crest for the hedenbergite-ferrosilite series. Kuno (1955, fig. 1) assumes that the temperature of the crest must lie below the hedenbergite-ferrosilite minimum because members of the hedenbergite-ferrosilite solid-solution are found in the later fractions of the Skaergaard intrusion. However, these pyroxenes are magnesium-bearing and are part of the series crystallized in the one-pyroxene field. Kuno's assumption is therefore only tenable if one is prepared to accept the second hypothesis under consideration, i.e. that in the one-pyroxene field the solid-solution series minimum is at a higher temperature than the crest of the solvus, and it would not be logical to use his assumption to support this hypothesis.

The crest of the solvus lies only very slightly below the solidus for the

system diopside-clinoenstatite, and it is generally believed that the addition of other constituents would lower the solidus to a temperature at which it is intersected by the solvus, so that two pyroxenes would then exist in cotectic equilibrium. During iron enrichment these conditions would continue to prevail, but should the slope of the crest of the solvus exceed that of the solid-solution minimum, there would be a change in composition of the two pyroxene phases such that the calcium-rich phase would become poorer, and the calcium-poor phase richer, in calcium. The type of change would depend upon the slopes of each limb of the solvus, but there would be a tendency towards ultimate convergence at the crest of the solvus (cf. Barth, 1952, fig. 30). If the solvus were a dome-shaped surface with steep sides, the two converging trend-lines on the Ca:Mg:Fe diagram would be convex towards the diopside-hedenbergite and clinoenstatite-ferrosilite joins respectively.

In the Skaergaard case the augite trend is concave towards the diopside-hedenbergite join, the calcium-poor pyroxene trend is parallel to the clinoenstatite-ferrosilite join, and there is no sign of convergence of these trends. None of this evidence supports the simple conception of a domed solvus dipping more steeply towards the hedenbergite-ferrosilite join than does the crystallization surface, until instead of intersecting this surface it dips beneath it, at the limit of two-pyroxene crystallization. The general conception of a crystallization surface with a gentler slope than the two-pyroxene to one-pyroxene 'transition surface' drawn by Tsuboi (1949, fig. 6) would require the production of a single pyroxene at one side of the intersection of these surfaces, equal to the average composition of the two pyroxenes at the other side of the intersection. Until this can be shown to happen, the specific trend-lines of each pyroxene in the two-pyroxene field and the peculiarly calcic composition of the pyroxene in the one-pyroxene field must be explained ultimately by reference to the structure of the pyroxenes and the effect of other components, particularly the olivines, on their equilibrium relationships.

The augites plotted in fig. 2 show no change in calcium content at the limit of two-pyroxene crystallization, which can be drawn somewhere between nos. 8 and 9 (each containing 35 % Ca of total Ca+Mg+Fe). In the hypothetical pyroxene equilibrium diagrams in which the augite in the one-pyroxene field is depicted as crystallizing at a liquidus minimum, and that in the two-pyroxene field on the calcic limb of a solvus, the only explanation for the Skaergaard pyroxene relationships shown in fig. 2 must require this minimum to be in practically the same

position (with respect to Ca: (Mg+Fe) ratio) when it intersects the solvus as when it leaves it. When basaltic magmas equivalent in composition to the earlier Skaergaard liquids crystallize to give one pyroxene, such as the sub-calcic augites, there is evidence for a liquidus minimum close to the line Ca: (Mg+Fe) = 25:75 (Kuno, 1955, figs. 2 and 7). This suggests that, during the fractionation of the Skaergaard magma, the minimum of the liquidus curves joining calcium-rich and calcium-poor pyroxenes in equilibrium moved towards the calcic component. The trace of this minimum on the Ca:Mg:Fe diagram (the 'two-pyroxene boundary' of Tsuboi, 1932, and the 'cotectic' of Hess, 1941) would show a change from Ca 25 to Ca 35. This evidence for migration of the liquidus minimum supports Muir's hypothesis that the cessation of pigeonite crystallization might be attributed to a migration of this type rather than to the fall of the solvus crest below the liquidus minimum.

Sub-solidus exsolution and inversion. Certain patches and lamellae of one pyroxene in another, once thought to be inclusions or replacement textures, have been attributed by Hess (1941) and by Poldervaart and Hess (1951) to exsolution in the solid state. These workers showed that particular exsolution textures in the pyroxenes could be linked with various stages of fractionation of a basaltic magma. Similar textures are present in the pyroxenes of the Skaergaard intrusion, and were described briefly by Wager and Deer, some being attributed to exsolution (1939, pp. 81 and 83). Detailed investigation of these textures has now shown that they can be closely related to the cooling history of the Skaergaard intrusion.

Exsolution textures in augites may be lamellae of orthopyroxene or pigeonite (usually inverted to orthopyroxene). Owing to their narrowness it is impossible to tell which they have been, but from Buerger's work (Hess and Poldervaart, 1951, p. 481) it seems likely that exsolution lamellae of orthorhombic in monoclinic pyroxene (and vice versa) will be || (100) while exsolution lamellae of monoclinic in monoclinic pyroxene will be || (001). If this is so then it ought to be possible to distinguish between the exsolution lamellae of orthopyroxene and pigeonite in augite purely on the basis of orientation. One would expect, however, that the type of pyroxene exsolved from the augite would generally be the same as that present as a separate mineral in the same rock.

In the Skaergaard augites the exsolution lamellae are very thin (about 0·003 mm. and totalling about 5 % of each grain) and their only recognizable optical property is a low birefringence; they are therefore probably orthopyroxene, but some may have developed through

pigeonite inversion. The calcium-rich augites of the gabbro-picrite (no. 1, fig. 2) are free from exsolution lamellae, but other rocks from the border group containing orthopyroxene in addition to augite (e.g. perpendicular-felspar rock, no. 2A, fig. 2) show exsolution lamellae of orthopyroxene || (100) in the augite. The augites of the wavy-pyroxene rock and lower members of the lower olivine gabbros (e.g. 4390 to 4392) contain lamellae parallel to both (100) and (001). Continuing the fractionation sequence, the augites in the layered series, up to those ferrogabbros in which the calcium-poor pyroxene phase ceases to crystallize, contain lamellae || (001), presumably of inverted pigeonite. In the ferroaugites of the remaining ferrogabbros, no exsolution lamellae can be seen, although in those from the lower levels represented by nos. 8 and 9 (fig. 2) there is an interesting schillerization due to the presence of a few extremely thin exsolution lamellae || (001) (Wager and Deer, 1939, p. 81). The schiller is only detected by rotating in a plane normal to the plane of the lamellae, when distinctive interference colours in ordinary light (probably produced through a diffraction process) are seen at positions $3\frac{1}{2}°$ at each side of the plane of the lamellae. There is thus a continuous and gradual change in the character of the exsolution lamellae in the augites which, as shown below, can be related to the gradual change in character of the calcium-poor pyroxene.

The orthopyroxenes in the gabbro-picrite (no. 1A, fig. 2) and the perpendicular-felspar rock (no. 2A, fig. 2) contain the type of fine-scale augite lamellae || (100) figured by Hess and Phillips (1938, fig. 2) while the wavy-pyroxene rock and lower members of the lower olivine gabbros (4390 to 4392) contain orthopyroxenes with these lamellae, forming rims and irregular extensions to orthopyroxenes rich in blebs and broad lamellae (pl. XVI, fig. 4). In some sections there is a strong suggestion that this association is due to exsolution in pigeonite beginning in the centre, to which material exsolved from the outer fringes is added, so that when inversion takes place the orthopyroxene at the margins is free from the broader lamellae (pl. XVII, fig. 7). Moreover, the fine lamellae || (100) in the orthopyroxenes of the earlier perpendicular-felspar rock die out towards the margins. However, the presence of lamellae parallel to both (001) and (100) of the augite at this horizon suggests that both orthopyroxene and pigeonite may have been in equilibrium with augite at approximately this temperature, although if there is any order of crystallization implied by the textures of the calcium-poor phase one would have expected the inverted pigeonite to rim the orthopyroxene.

The prevalent calcium-poor pyroxene of the layered series is a pigeonite, which has usually inverted on cooling to an orthopyroxene. It is classed as a pigeonite because of its calcium-content (9 % Ca of total Ca+Mg+Fe; see Poldervaart and Hess, 1951, p. 482) and, in the rare cases where it has not inverted, by its low positive 2V (16°). The presence of 9 % calcium is proven by chemical analysis of three examples, and supported by measurement of the proportion of exsolution lamellae of augite (usually 20 %) in orientated grains. Poldervaart and Hess (1951, p. 482) have suggested that most lamellae exsolved from pigeonite are ‖ (001) and that upon inversion these lamellae as well as the simple (100) twin plane are preserved in the host orthopyroxene, the grain retaining the 'herringbone twin' structure characteristic of monoclinic rather than orthorhombic minerals. This was verified in Skaergaard examples by measurement of the angle (001):(100), for the β angle in pigeonite has been determined from X-ray spectrograms (Kuno and Hess, 1953) and is approximately $71\frac{1}{2}°$. In certain cases it was possible to use this method as a further check on the Skaergaard inverted pigeonites, but, as will be shown below, the occasional lack of lamellae parallel to (001), the scarcity of preserved twin planes, and the frequent failure of the orthopyroxene to retain the *b* and *c* crystallographic axes of the parent pigeonite on inversion meant that this method was of limited value.

Although pigeonite occurs in the inverted form throughout a great thickness of the layered series, reference to fig. 5 will indicate that there is likely to be a great deal of variation in the conditions under which the exsolution of augite and inversion to orthopyroxene takes place. From the point at which the crystallization curve passes above the inversion curve, falling temperature and iron enrichment widen the gap between the two curves. This means, assuming a fairly constant rate of cooling, a progressive increase in the period available for exsolution prior to inversion and therefore an increase in the opportunity for ordered arrangement of the exsolved augite within the pigeonite structure before the latter inverts to the orthorhombic form. This is borne out by the Skaergaard inverted pigeonites, for in the lower olivine gabbros they contain exsolved augite as irregular blebs thrown out of the orthopyroxene which probably formed before they could be arranged as lamellae parallel to distinct structural planes in the pigeonite (i.e. not due to rapid cooling only, as suggested by Poldervaart and Hess, 1951, p. 482). Upward in the sequence lamellae develop in place of the blebs, at first incomplete and irregular (pl. XVII, fig. 6), but finally (in the middle gabbros) becoming regular, fully traversing each grain (pl. XVII, fig. 8).

Most of the broader lamellae exsolved from pigeonite are about 0·01 mm. thick and 0·04 mm. apart, in contrast to the fine-scale lamellae of the host orthopyroxene, less than 0·001 mm. thick. Despite the variation in pigeonite exsolution textures now to be considered, a generalized diagram (fig. 6) can be used to show the orientation and general character of the exsolution lamellae in the ideal case where the *b*- and *c*-axes of pigeonite are retained, on inversion, by the orthopyroxene.

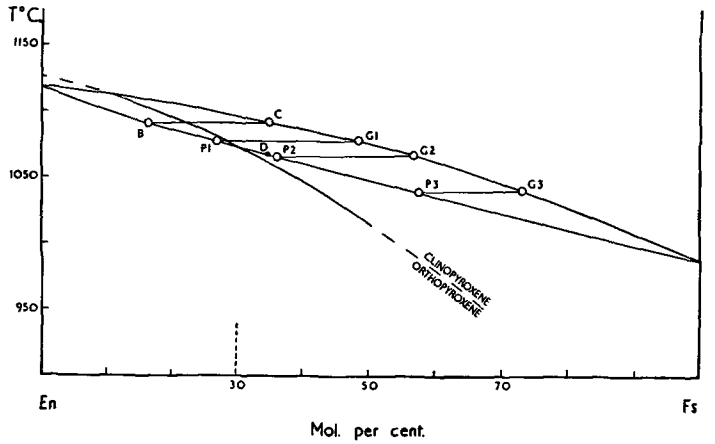

FIG. 5. Possible relationship between the crystallization curve of calcium-poor pyroxenes and the inversion curve (see Appendix). D = pigeonite of chilled marginal gabbro (4507), Skaergaard intrusion; B = bronzite of gabbro-picrite (4526), Skaergaard intrusion, crystallized at temperature (C); P1, G1, . . . = coexisting phenocryst and groundmass pyroxenes of Japanese lavas (Kuno, 1950).

In the chilled margin the inverted pigeonite (now orthopyroxene, Fe_{37}, through exsolution of augite) contains fine lamellae || (001) and (100) and irregular patchy plates || (010). In the lower rocks of the lower olivine gabbros, e.g. 4392, the inverted pigeonite (now orthopyroxene, Fe_{37}, no. 3A, fig. 2) contains no lamellae || (001), but large blebs || (010), short broad lamellae || (100), and, rarely, the better-known fine-scale lamellae || (100) occur in the host orthopyroxene (pl. XVI, fig. 4). The blebs in a single grain of orthopyroxene are in optical continuity with one another, but the optical orientation of sets of blebs, in relation to that of their host orthopyroxene, is extremely variable from grain to grain and shows no order. Also in a single grain the optical orientation of the augite in the blebs is different from that in the augite of the broader (100) plates. The 'blebs' are really small plates and in sections

|| (010) frequently show elongation || (100), though they rarely extend beyond 20 % of the width of the host mineral. In pigeonites from higher rocks of the lower olivine gabbros, such as 4385A (now orthopyroxenes, Fe_{39}, no. 4A, fig. 2), lamellae begin to develop || (001). However, these lamellae rarely extend more than half the width of the grain and are occasionally bleb-like when viewed in sections || (001) (pl. XVI, fig. 2). Leading from the lamellae, as seen in (010) sections, are narrow lamellae || (100), but these do not resemble the narrow fine-scale lamellae seen in orthopyroxenes of the marginal border group and common in bronzites of the Bushveld and Stillwater intrusions. They are short, merely linking adjacent (001) lamellae (cf. Wager and Deer, 1939, p. 83), whereas those in some of the lower inverted pigeonites are parallel and can be joined at each side of the (001) lamellae. This suggests that the shorter (100) lamellae were exsolved from the pigeonite rather than from the orthopyroxene subsequent to inversion, although both types may be present (pl. XVI, fig. 4). Abundant opaque ore inclusions distinguish inverted pigeonite from augite in ordinary light and are probably released upon inversion to orthopyroxene (hence their lack of orientation). The pigeonite contains less Fe‴ than the augite (table II), while this textural evidence suggests that the orthopyroxene contains even less Fe‴ than the pigeonite.

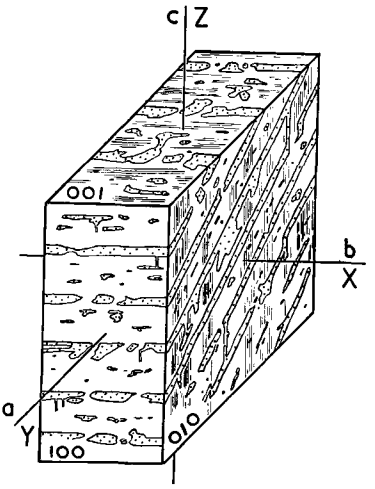

FIG. 6. An inverted pigeonite with the common exsolution lamellae of augite (stippled and fine lines) now in orthopyroxene. The broad lamellae (0·01 mm. thick and 0·04 mm. apart) are parallel to (001) and, though less common and complete, parallel to (100) and (010) of the original pigeonite. The more regular, narrow lamellae (0·001 mm. thick) are parallel to (100) of the host orthopyroxene. The example drawn is a generalized case in which the *b* and *c* crystallographic axes of the pigeonite are retained, upon inversion, by the orthopyroxene, and in which the degree of exsolution is extreme. The crystallographic and optic directions shown apply to the orthopyroxene host.

In the middle gabbros and lower ferrogabbros the exsolution lamellae in the inverted pigeonites are broad, well developed, and fully traverse each grain. Between each pair of lamellae is a string of tiny blebs that

appear to be exsolved augite, in insufficient quantity to form lamellae but spread along the (001) plane (pl. XVII, fig. 8). There are also abundant fine-scale lamellae || (100), which together with the (001) lamellae and blebs make the determination of optic axial angle, refractive index, and unit-cell dimensions of the host orthopyroxene difficult. The compositions of the host orthopyroxenes (4B, 6B, 7B, of fig. 2) of the inverted pigeonites indicate that the exsolved augite is more ferriferous in composition than the augite existing as a separate phase in the same rock.

Poldervaart and Hess (1951, p. 482 and fig. 7) have observed that 'in the great majority of cases of inversion of pigeonite to orthopyroxene, the orthopyroxene will develop in such an orientation that it retains the *b* and *c* crystallographic axes of the parent-pigeonite'. In exceptional cases, they remark, a rotation of *c* through 45° has been recorded. In the case of the Skaergaard inverted pigeonites the reverse is true, for it is rare to find the orthopyroxene host retaining either *b*- or *c*-axes of the parent pigeonite. It is clear from textural evidence that augite and pigeonite, when adjacent, crystallized so as to share the three major crystallographic axes. This is shown by the optical continuity between augite plates exsolved from pigeonite and adjacent augite crystals, and even more convincingly in the relationship illustrated by pl. XVI, fig. 2: a twinned augite has been poikilitically enclosed by pigeonite, the latter crystallographically continuous to the extent of reproducing the twinned structure; the pigeonite has subsequently exsolved augite lamellae (bleb-like in this basal section), which have in turn crystallized in continuity with the twinned pigeonite (finally inverted). The final result superficially suggests that the central twinned augite has exerted a complex influence on the growth of the two sets of blebs, but this is not directly true, for the role of pigeonite must be included in the process. However, when the augite blebs in the inverted pigeonite from rocks such as 4392 are considered (p. 530), it is clear that the relationship between the orientations of host orthopyroxene and augite blebs varies from one grain of inverted pigeonite to the next. If the augite retains the crystallographic orientation of the pigeonite (and there is plenty of evidence of the type cited above to support this suggestion) then the host orthopyroxene cannot be retaining the *b*- and *c*-axes of the parent pigeonite, otherwise the *b*- and *c*-axes of host orthopyroxene and exsolved augite would also correspond.

Further evidence on this point was obtained when a stereographic plot was made of the *a*-, *b*-, and *c*-axes of the host orthopyroxene and

the pole of the broad exsolution plates from a number of inverted pigeonites at representative horizons within the Skaergaard intrusion. From this it had been hoped, initially, to record the planes in the parent pigeonite along which exsolution developed prior to inversion. Several poles of exsolution lamellae fell on a point in the stereogram represented by β 71½° (approx.), provided that the *b*- and *c*- axes in pigeonite and orthopyroxene are assumed to be shared, and as these poles correspond to the pole of (001) in pigeonite it is likely that the axes are, in fact, shared. However, the poles of the broad lamellae from other grains fell in random positions on the plot and showed no concentrations. This is interpreted as implying that the lamellae represent neither random inclusions nor various important crystallographic planes within the pigeonite, but that they were parallel to (001) of the parent pigeonite, and that upon inversion the orthopyroxene has become randomly orientated so as to retain neither the *b*- nor the *c*-axes of the parent pigeonite. If this is true then it is impossible to tell which plane of a parent pigeonite is represented by a particular set of exsolution lamellae, merely by relating these lamellae to the optic axial plane of the host orthopyroxene. However, it can be done by using the relict (100) twin plane in conjunction with lamellae, if the former is preserved. A grain examined in this way (pl. XVII, fig. 9) shows the (100) twin plane and (001) exsolution lamellae as relict structures of the parent pigeonite, as proven by a measurement of β (orientated on the universal stage). Yet in the same grain can be seen fine-scale augite lamellae parallel to the optic axial plane, (100), of the host orthopyroxene that are far from parallel to the (100) twin plane of the parent pigeonite. Rotation about both *b*- and *c*-axes is involved in this inversion. Further evidence is brought by the numerous cases, especially at the middle gabbro horizon, in which a single crystal of pigeonite has inverted to two or more crystals of orthopyroxene, optically discontinuous with one another (pl. XVI, fig. 3). Even if one of these crystals retained the *b*- and *c*-axes of the parent pigeonite the other(s) could not. Measurement of one such inverted pigeonite from the top of the lower olivine gabbros (4378) showed that from one orthopyroxene to the next γ was rotated through 100° about a pole (*hk*0) at an angle of 32° from *a* and 68° from *b*. Although it was not possible to obtain more measurements of this type, the one example proves that even if one orthopyroxene retained *b* and *c* of the parent pigeonite, the other shows rotation about both *b*- and *c*-axes. Together with the rest of the evidence given, it seems most likely that upon inversion the retention of *b*- and *c*-axes, or rotation with reference to one or both, is a random process.

The proportion of grains of inverted pigeonite that show rotation rather than retention of axes on inversion increases with iron content and is most marked in the middle gabbros (pigeonites now orthopyroxenes, Fe_{47-50}). Bowen and Schairer (1935, p. 164 and fig. 8) investigated synthetically the inversion relationships between monoclinic and orthorhombic pyroxenes, although they could only do this in the direction orthorhombic to monoclinic, on heating. In doing so they pointed out (1935, p. 169) that although in the more magnesian members there is a tendency towards the retention of the prism zone, 'In general, a single crystal or crystal fragment of orthorhombic pyroxene is transformed into an aggregate of several grains of monoclinic pyroxene of random orientation with respect to each other and to the original orthorhombic substance.' In reverse, this is what has happened to the Skaergaard pigeonites on inversion, those with an intermediate composition showing the phenomenon more markedly than the more magnesian members. Bowen and Schairer (1935, p. 167) cite further experimental evidence in support of this fact, for while the members approaching the two ends of the series are transformed readily, the intermediate members behave much more sluggishly. It is possible that this sluggishness is because of the inability of the intermediate members to grow, upon inversion, with the orientation of the parent mineral. Moreover, the presence of rare grains of uninverted pigeonite and partially inverted pigeonite amongst these intermediate members alone is probably due to the sluggishness of inversion at a stage when an appreciable interval separates the temperatures of crystallization and inversion (fig. 5). The inversion curve for the intermediate and ferriferous pigeonites is, in fact, likely to fall to temperatures at which processes involving significant rearrangement of the pyroxene structure will become increasingly difficult at the rate of cooling of fairly high-level, small intrusions.

Optical properties in relation to chemical composition. The most reliable method at present of determining the Ca:Mg:Fe ratio of a calcic clinopyroxene from the optical properties is to determine $2V_\gamma$ by direct rotation between optic axes and β refractive index on (100) parting tablets, using techniques and determinative curves similar to those given by Hess (1949). For the analysed Skaergaard augites these techniques were used and only $2V_\gamma$ and β refractive index were determined as these are the significant diagnostic optical properties.

In comparing the optical properties of an augite with the composition it is necessary to bear in mind the effect on the optics of factors other

than the Ca:Mg:Fe ratio, chief of which are the degree of exsolution of calcium-poor pyroxene (which mainly affects 2V) and the amount of minor constituents such as Al and Ti (which affects both 2V and refractive index).

Through exsolution of orthopyroxene or pigeonite the optic axial angle measured will be that of the host augite and will not correspond to the augite represented by the bulk composition. The discrepancy between 2V of augite before and after exsolution of calcium-poor pyroxene will vary with the amount and composition of the exsolved material. The amount will be controlled by the rate of cooling of the rock below the temperature of augite crystallization and the initial composition of the augite (exsolution will cease when, or perhaps a little before, the host augite attains the composition of diopside-hedenbergite). The composition of the exsolved material may be either orthopyroxene or pigeonite, but if a calcium-poor pyroxene ceases to form as a crystal phase in equilibrium with the magma (as in the case of most of the Skaergaard ferrogabbros) then it is unlikely that there will be exsolution of this phase from the augites.

Variable 2V in a single grain, often classed as 'zoning' (i.e. variation chiefly in Fe:Mg ratio), is more likely to be a function of irregular Ca distribution and may be due to exsolution being variable in extent throughout the grain.

If use is to be made of the correlation between optical properties and chemical composition of pyroxenes, it is essential that the composition and quantity of the exsolved phase be estimated and taken into account in compiling determinative tables and curves. In the case of the Skaergaard pyroxenes there are no exsolution lamellae in the diopsidic augite of the gabbro-picrite (because of its calcic composition) and in the ferroaugites of most of the ferrogabbros (because of the instability of pigeonite). In the other analysed augites the exsolution lamellae are of inverted pigeonite (see p. 528) amounting to approximately 5 % of each crystal. The composition of the exsolved phase is assumed to be that of the inverted pigeonite present as a separate phase in the same rock, and although this is only an approximation it is the most likely assumption. Using the compositions given in table I a close approximation to the composition of the host augite is obtained (table III) and these are the compositions used in compiling fig. 7. Ultimately it should be possible to derive the composition of the host augite in terms of Ca, Mg, and Fe from unit-cell dimensions (providing the unit-cell determinative curves are initially constructed using augites free from exsolution lamellae,

possibly homogenized by heating), and relate this composition to the optical properties of the host augite. However, the calcium-poor pyroxene also contains smaller amounts of Al, Fe‴, Ti, Cr, and Na than the augite (table II and p. 518) and when more is known about the effect of these constituents on the optical properties of augites the composition of the host augite must be more accurately determined.

When the compositions of the Skaergaard augites have been corrected for exsolution and plotted on Hess's curves (1949, pl. I) they correspond to a 2V about 7° in excess of that observed, whereas when plotted uncorrected for exsolution the 2V is about 4° in excess of that observed.

TABLE III. Composition of analysed augites (atomic %) recalculated to give approximate composition of augite free from 5 % exsolution lamellae of pigeonite. (Specimen numbers refer to the analyses of table I.)

	3.	4.	5.	6.	7.	8.	9.
Ca	41	39	38	37	36	36	36
Mg	42·5	41	39	37·5	37	35	32
Fe	16·5	20	23	25·5	27	29	32

This suggests that certain parts of Hess's curves correspond more closely to the composition of host plus lamellae than to host, and that a better estimate of composition is obtained if 3° is added to the 2V observed (cf. Brown, 1956, pp. 25 and 51) rather than subtracted as suggested by Hess (1949, p. 636). Moreover, some of the augites used by Hess may contain more or less than 5 % exsolved pigeonite, and until further details are available on the composition and quantity of exsolved material in each case, comparisons must be tentative.

The remaining discrepancy of 4° between the observed 2V and that calculated from Hess's curves can best be explained by a brief consideration of the effect on the optics of cations other than Ca, Mg, and Fe. The effect of minor constituent cations on the optical properties of augites was appreciated by Hess (1949, p. 633) but Segnit (1953) was the first to determine the effect of Ti, Al, and Fe‴ on the optical properties of a clinopyroxene, in this case synthetic diopside; he found that Al has little effect on the refractive index but increases 2V; Ti and Fe‴ increase both refractive index and 2V. An important point noted by Hori (1954, p. 73), however, is that the effect of a cation on optical properties is dependent upon its lattice site, and that Al, Ti, and Fe‴ in tetrahedral coordination decrease the refractive index and increase 2V, whereas in octahedral positions they have the opposite effect (marked in the case of Ti). The Skaergaard augites contain average amounts of Al_2O_3 (*ca.* 2·5 %)

and Fe_2O_3 (*ca.* 1·5 %) but contain almost 1 % TiO_2 (average 0·4 %, see Hess, 1949, p. 643). In nearly every case this excess Ti is accommodated in the octahedral position (table II), which would account for the 2V being lower than that of augites of otherwise similar composition, even after exsolution has been taken into account.

When the curves for the β refractive index of the Skaergaard augites are considered, it is seen that for specific Ca:Mg:Fe values they read

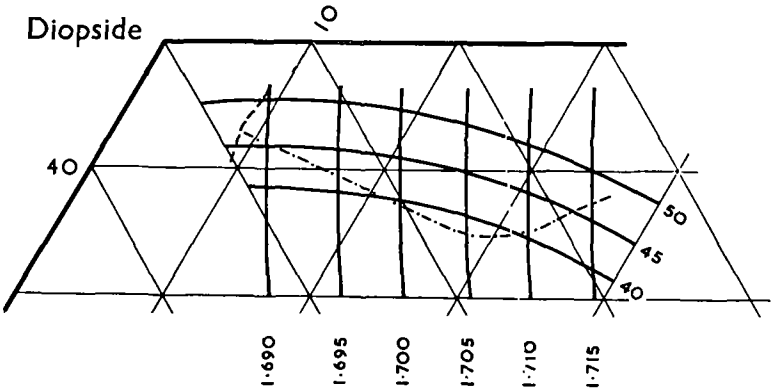

FIG. 7. Relationship between optical properties and chemical compositions of the Skaergaard augites. Composition corrected, where necessary, for exsolution (see table III). ⌒ optic axial angle; (β refractive index; – · · · – crystallization trend-line; – – – position of the 1·690 β curve for chromiferous augites.

0·005 higher than those of Hess (1949, pl. I). The higher value for the Skaergaard augites might also be explained by the presence of Ti in the octahedral position, in view of Hori's hypothesis. In fact, when augite analyses nos. 28 to 33 of Hess (1949) are examined they are found to resemble the Skaergaard augites in many respects, particularly in both TiO_2 content (all Ti being in the octahedral position) and in the fact that their observed β refractive indices are usually 0·005 higher than those calculated from the curves. The effect of Cr on the refractive indices has been estimated by Hess (1949, pl. I) and an allowance has been made for this constituent in fig. 7.

In view of the problems involved in dealing with so many variable factors, the simple Ca:Mg:Fe diagram is inadequate as a means of representing the optical properties of augites. Fresh curves have been drawn on such a diagram for the Skaergaard augites, chiefly to indicate how their value is limited to the estimation, from optical properties, of

the composition of the unanalysed members of a series of augites in a fractionated series, providing the nature of the sub-solidus exsolution textures is understood and the distribution of minor cations is fairly constant throughout the series. To apply to these curves the optical properties of augites crystallizing from magmas of different composition and cooling history from the Skaergaard magma, in order to estimate their composition, is bound to produce anomalous results.

The ferroaugites free from exsolution lamellae will be described in a future paper, and fresh curves will be drawn for this region. Muir (1951, fig. 4) has drawn curves (2V and β) for the ferroaugite region but these do not correspond with his recorded compositions and optical properties (1951, table II), while the trend of augite–ferroaugite crystallization towards hedenbergite is also based upon an erroneous application of observed optical properties to these curves.

The compositions of the orthopyroxenes, including those formed by inversion, were determined by measurement of $2V_\alpha$ and γ, using Hess's curves (1952, fig. 2).

Conclusions. Two pyroxenes, a calcium-rich and a calcium-poor variety, crystallized from the Skaergaard magma before fractionation began, and continued to crystallize together during fractionation until the latest stages, represented by the upper 900 m. of the exposed layered series, when the calcium-poor variety ceased to crystallize (fig. 1).

The calcium-rich variety is an augite, which changed composition with fractionation, at first by the replacement of Ca and Mg by Fe″, the slope of the trend-line being such that for (approximately) every seven Fe″ atoms gained, three Ca and four Mg atoms were lost; the loss of Ca reached a limit when Ca:(Mg+Fe) equalled 35:65, the compositions of the augites from the following 250 m. of rock changing through replacement of Mg by Fe″, without any change in the Ca percentage of 35; above (and partly within) this zone, augite crystallized as the only pyroxene and now changed composition by the replacement of Mg by both Ca and Fe″ (fig. 2).

The earliest calcium-poor pyroxene to crystallize through fractionation was an orthopyroxene, which changed composition through the replacement of Mg by Fe″. Later a pigeonite crystallized instead of orthopyroxene and also changed composition, during cooling of the Skaergaard magma, through the replacement of Mg by Fe″, the Ca content remaining constant at 9 % of Ca+Mg+Fe. The changeover from orthopyroxene to pigeonite crystallization took place between Mg:Fe =

72:28 and 63:37 (hidden layered series), while the cessation of pigeonite crystallization occurred near the composition Mg:Fe = 45:55 (fig. 2). The limit of two-pyroxene crystallization is thought to be reached when the liquidus minimum for the pyroxene system has migrated to the calcium-rich limb of the solvus, i.e. from about Ca 25 to Ca 35 in the Ca:Mg:Fe diagram.

The trend of crystallization of both calcium-rich and calcium-poor pyroxenes from the Skaergaard is, in the early and middle stages, similar to the less complete trends followed by the pyroxenes from other layered basic intrusions of the Bushveld–Stillwater type. If, however, the pyroxenes of the Skaergaard gabbro-picrite represent the earliest pyroxene fractions, their composition suggests the Skaergaard magma was cooler, or further advanced along the tholeiitic-basalt fractionation trend, than the Bushveld, Stillwater, and Rhum magmas (fig. 3).

The compositions of the inverted pigeonite of the chilled marginal gabbro and the orthopyroxene of the early-accumulate gabbro-picrite are believed to be related in the same way as the groundmass and intratelluric phenocryst pyroxenes of lavas. They are used to construct a diagram that explains the relationship between the liquidus and solidus cooling curves and the monoclinic to orthorhombic inversion curves of calcium-poor pyroxenes. The diagram, as constructed, indicates supercooling of at least 20° C. at the chilled margin, and crystallization of most of the Skaergaard intrusion within a temperature range of 50° C. (fig. 4).

Both calcium-rich and calcium-poor pyroxenes contain sub-solidus exsolution textures, the orientation and thickness of which can be related to the composition of the host pyroxene so accurately that it is possible to estimate the horizon from which a specimen was collected, purely on the basis of these textures. The majority of the pigeonites have inverted to orthopyroxene, but before and after inversion augite lamellae were exsolved from the crystals. These lamellae, beginning as blebs, become progressively more ordered and abundant with height in the layered series, and this is related to the progressive increase in the temperature interval between crystallization and inversion. At the same time it is believed that the inversion of pigeonite to orthopyroxene became progressively more difficult with height in the layered series, because the *b* and *c* crystallographic axes of the pigeonite are not always retained by the orthopyroxene on inversion, the proportion of grains showing non-retention of axes increasing with height in the series; in the few hundred metres before it ceased to crystallize altogether pigeonite

has failed to invert, at first only partially in each grain, but ultimately the whole grain remains as pigeonite.

In the past the presence of uninverted pigeonite and of 'blebby' inverted pigeonite have been attributed to quick cooling of the magma. The fact that these two phenomena occur at quite separate horizons in the Skaergaard intrusion and can be traced through gradual changes into the other varieties attributed to slow cooling, together with the more evident geological relationships, rule out the quick-cooling hypothesis. The rate of cooling must have been relatively constant, but the temperature interval, and therefore the time interval, between crystallization and inversion curves increased as cooling proceeded. Thus the time for ordered and plentiful exsolution would slowly increase while the time for inversion would slowly decrease (fig. 5).

It is evident that the degree of inversion of the pigeonitic pyroxenes, and possibly the high-transitional-low temperature form of the associated plagioclase felspars (cf. Muir, 1955) must, in general, be correlated with the composition of the minerals as well as with their cooling history.

The chemical analyses of the pyroxenes show that elements other than Ca, Mg, and Fe″ change in amount during fractionation. Of particular interest is the progressive decrease in Al, the evidence that Ti is not so abundant as indicated by previous investigators, and the enrichment of the calcium-rich pyroxene, relative to the calcium-poor pyroxene in the same rock, in Al, Fe‴, Ti, Na, and Cr.

Fresh optics curves are drawn for the Skaergaard clinopyroxenes in the range investigated, but these must be used with caution in view of the effect on the optics of exsolution, of cations other than Ca, Mg, and Fe″, and of the lattice site occupied by these cations in the pyroxene structure.

Acknowledgements. The material used in this investigation was collected during the East Greenland Geological Expedition, 1953, led by Prof. L. R. Wager and Prof. W. A. Deer, of which the author was a member. The leaders thank the Royal Society and the Percy Sladen trustees for generous financial assistance.

The author wishes to thank Prof. Wager for much help with the planning and final presentation of the work, and interpretation of some of the results. In particular he was concerned with the examination of primary crystallization textures, and the recognition of the significance of inverted pigeonite in the chilled marginal gabbro.

Thanks are also expressed to Prof. H. H. Hess of Princeton University for useful discussion and facilities granted for part of this study, and to Prof. Deer for making available the two analyses by Dr. P. E. Brown. A Fellowship from the Commonwealth Fund of New York, for study at Princeton, is gratefully acknowledged.

Appendix.

In constructing fig. 5 reference was made to a similar one for a pigeonitic rock series drawn by Kuno (1950, fig. 24, p. 997) and later modified by Kuno and Nagashima (1952, fig. 1) in which phenocrysts from lavas were plotted on the solidus and groundmass pyroxenes on the liquidus. Kuno's diagram could not be used directly, however, because of several assumptions made in constructing his diagram which were not easily explained: no temperatures were recorded by Kuno on the ordinate; the slope of the inversion curve, attributed to Bowen and Schairer (1935), is adapted to the results obtained by Kuno without explanation (more evident in Kuno and Nagashima's diagram, where temperatures are stipulated); the diagram is complicated by a large inversion interval, despite Bowen and Schairer's statement (1935, p. 170) that the inversion interval of temperature is 'vanishingly small' and Kuno and Nagashima's evidence (1952, fig. 2) that the inversion interval of composition (as a function of En : Fs ratio) is negligible; the solidus is assumed to approach the liquidus when the groundmass pyroxene crystallizes, in order to explain the changeover from hypersthene to pigeonite. The two critical pyroxenes illustrating the Skaergaard case (p. 520) cannot therefore be plotted on this diagram and a new one was constructed to illustrate this particular case.

The three examples given by Kuno (fig. 24) were plotted (1, 2, 3), with the aid of the ordinate temperature scale by Kuno and Nagashima (1952, fig. 1), together with the inverted pigeonite from the Skaergaard chilled marginal gabbro (C) and the orthopyroxene from the Skaergaard early-accumulate gabbro-picrite (B). Each set fell on a smooth liquidus and solidus line, from which it was assumed that no difference in the relationship between solidus and liquidus existed for plutonic and volcanic rocks. In selecting an appropriate temperature of crystallization for the Skaergaard pyroxenes, reference was made to the results of experiments by Yoder and Tilley (1956, p. 100), who heated Kilauean tholeiitic basalt at 5000 bars water pressure; at 1090° C. pyroxene disappeared. In the absence of more precise figures it is assumed that pyroxenes began to crystallize from the Skaergaard magma at approximately this temperature. If the curves are applicable, the development of pigeonite, subsequently inverted, in the chilled marginal gabbro indicates supercooling of the order of 20° C. Moreover the crystallization of a calcium-poor pyroxene of composition approximately $En_{45}Fs_{55}$ (reduced to Ca-free proportions) at a level of 1900 m. suggests that most of the Skaergaard intrusion (i.e. border group + hidden layered series + $\frac{2}{3}$ exposed layered series) crystallized within a temperature range of about 50° C.

In the construction of this type of diagram, applied to natural magmas, it is not practical to retain, without slight modification, the clinopyroxene-orthopyroxene inversion curve determined by Bowen and Schairer for the simple dry system. It seems most likely that under natural conditions, in the presence of fluxes, inversion takes place at lower temperatures. The curve is therefore dropped and the shape changed slightly in order to intersect the solidus at Fs_{30}, where the changeover from orthopyroxene to pigeonite crystallization was observed to take place in lavas (Kuno and Nagashima, 1952). The precise point of intersection will vary according to the temperatures and compositions of the magmas, some extreme cases having been described by Muir (1954), but from fig. 5 it is clear that only very slight adjustment of the curves is necessary in order to bring the intersection to Fs_{40}, when the conditions of crystallization of pyroxenes from several basalts, rather than from gabbros, are represented.

References.

ATLAS (L.), 1952. Journ. Geol., Chicago, vol. 60, p. 125 [M.A. **12**–80].
BARTH (T. F. W.), 1952. Theoretical Petrology. 1st edn., p. 110. John Wiley and Sons, New York.
BOWEN (N. L.), 1914. Amer. Journ. Sci., ser. 4, vol. 38, p. 207.
—— and SCHAIRER (J. F.), 1935. Ibid., ser. 5, vol. 29, p. 151 [M.A. **6**–352].
——, SCHAIRER (J. F.), and POSNJAK (E.), 1933. Ibid., vol. 26, p. 193 [M.A. **5**–454].
BROWN (G. M.), 1956. Phil. Trans. Roy. Soc., ser. B, vol. 240, p. 1.
BROWN (P. E.), 1955. Ferromagnesian Minerals of the Skaergaard Intrusion, East Greenland. Ph.D. thesis (unpublished), University of Manchester.
HESS (H. H.), 1941. Amer. Min., vol. 26, pp. 515, 573 [M.A. **8**–233].
—— 1949. Ibid., vol. 34, p. 621 [M.A. **11**–15].
—— 1952. Amer. Journ. Sci., Bowen vol., p. 173 [M.A. **12**–97].
—— and PHILLIPS (A. H.), 1938. Amer. Min., vol. 23, p. 450 [M.A. **7**–180].
HORI (F.), 1954. Sci. Papers College Gen. Education, Univ. Tokyo, vol. 4, no. 1, p. 71.
KUNO (H.), 1955. Amer. Min., vol. 40, p. 70.
—— and HESS (H. H.), 1953. Amer. Journ. Sci., vol. 251, p. 741 [M.A. **12**–334].
—— and NAGASHIMA (K.), 1952. Amer. Min., vol. 37, p. 1000 [M.A. **12**–138].
MUIR (I. D.), 1951. Min. Mag., vol. 29, p. 690.
—— 1954. Ibid., vol. 30, p. 376.
—— 1955. Ibid., vol. 30, p. 545.
POLDERVAART (A.) and HESS (H. H.), 1951. Journ. Geol., Chicago, vol. 59, p. 472 [M.A. **11**–290].
SEGNIT (E. R.), 1953. Min. Mag., vol. 30, p. 218.
TSUBOI (S.), 1932. Japan. Journ. Geol. Geogr., vol. 10, p. 67 [M.A. **5**–219].
—— 1949. Proc. Japan. Acad., vol. 25, no. 1, p. 34.
WAGER (L. R.) and DEER (W. A.), 1939. Medd. Grønland, vol. 105, no. 4, p. 1 [M.A. **11**–32].
WILKINSON (J. F. G.), 1956. Amer. Min., vol. 41, p. 724.
YODER (H. S.) and TILLEY (C. E.), 1956. Program 1956 Annual Meetings, Geol. Soc. Amer., p. 100.

EXPLANATION OF PLATES XVI AND XVII.

(Specimen numbers refer to rocks in the Oxford University East Greenland Collection.)

PLATE XVI.

FIG. 1. Inverted pigeonite approximately || (010). Augite has been exsolved as broad, irregular plates || (010) (in optical continuity with augite crystal in bottom right-hand corner), long lamellae || (001), and short lamellae || (100). Orthopyroxene host at extinction. Crossed nicols. ×70. (E.G. 4454. Height 1050 m.)

FIG. 2. Twinned crystal of augite poikilitically enclosed by pigeonite. The pigeonite has grown in structural continuity with the augite, reproducing the twinned structure. The pigeonite has then exsolved blebs of augite, each set being in structural continuity with that part of the pigeonite twin from which they were exsolved. Finally, inversion of pigeonite to orthopyroxene has destroyed evidence of the twin structure in the poikilitic host mineral (shown at extinction). Crossed nicols. ×24. (E.G. 5062. Height 300 m.)

FIG. 3. Inverted pigeonite approximately || (010). One twinned crystal has inverted to two crystals of orthopyroxene, one of which is at extinction. Crossed nicols. ×62. (E.G. 4378 B.)

FIG. 4. Inverted pigeonite, section approximately || (010). Augite has been exsolved from the pigeonite, prior to inversion, as blebs || (010) and short thick lamellae || (100), and from the orthopyroxene host, subsequent to inversion, as very fine-scale lamellae || (100). Crossed nicols. ×52. (E.G. 4392.)

FIG. 5. Inverted pigeonite approximately || (010). Broad lamellae are || (001) of the original pigeonite, while the fine lamellae running from top to base of picture are || (100) of the host orthopyroxene (shown at extinction). The angle between the two sets of lamellae proves that the (100) planes of pigeonite and orthopyroxene do not coincide. The irregular exsolution running approximately left–right typifies the more complex patterns to be found. Crossed nicols. ×100. (E.G. 4385 B.)

PLATE XVII.

FIG. 6. Inverted pigeonite approximately || (010). Augite has been exsolved || (001) of a pigeonite twinned on (100). Small fine lamellae can be seen joining some of the broad (001) lamellae. Orthopyroxene host at extinction. Crossed nicols. ×26. (E.G. 4386.)

FIG. 7. Inverted pigeonite interstitial to olivine, augite, and plagioclase. Augite has been exsolved first from the centre, material migrating there from the margins. The symmetrical arrangement of orthopyroxene (shown at extinction) free from exsolved augite at each margin indicates that the orthopyroxene has not grown as a later rim to the pigeonite. Crossed nicols. ×105. (E.G. 4391 B.)

FIG. 8. Inverted pigeonite as distinct primary precipitate crystals in the middle gabbros. The exsolved augite lamellae || (001) are well developed, while between them are stringers of augite blebs, indicating a high degree of augite exsolution prior to inversion. Orthopyroxene host at extinction. Crossed nicols. ×78. (E.G. 4369.)

FIG. 9. Inverted pigeonite approximately || (010). The original (100) twin plane of the pigeonite is well defined by the herringbone texture (cf. Pl. XVII, fig. 6), but this does not correspond with the (100) plane of the host orthopyroxene, defined by the lamellae running from top to base of the picture. Crossed nicols. ×90. (E.G. 4378 B. Height 800 m.)

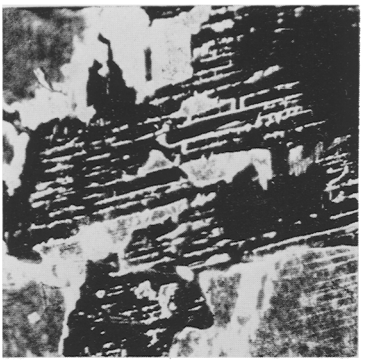

1

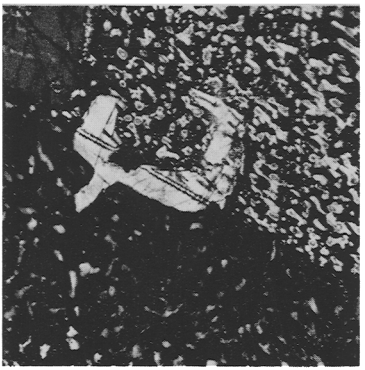

2

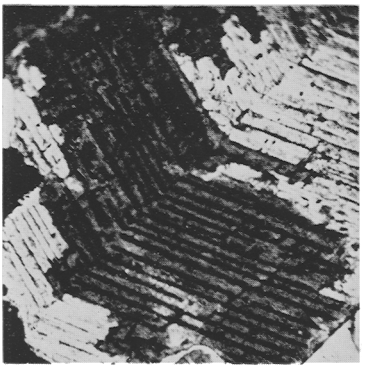

3

4

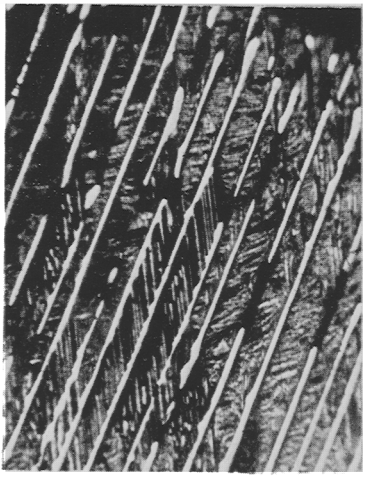

5

G. M. BROWN: PYROXENES

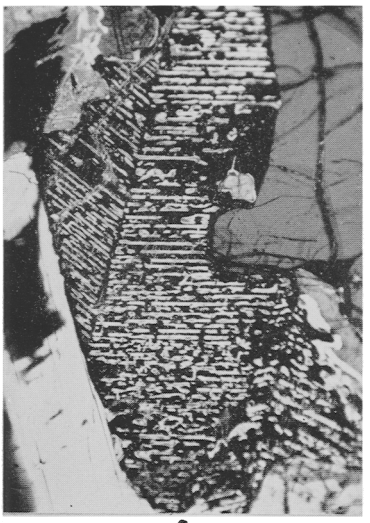

6

7

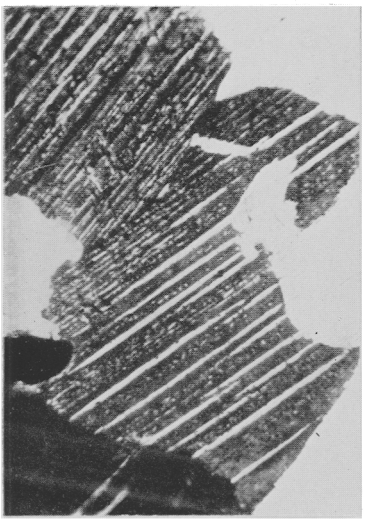

8

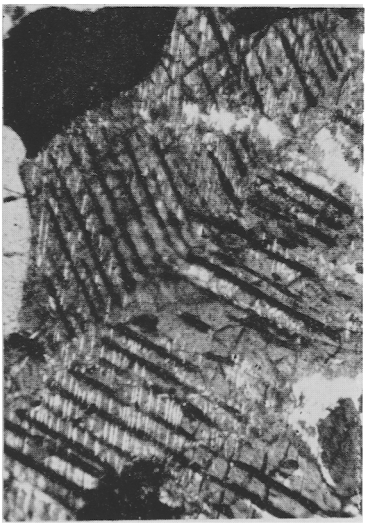

9

G. M. BROWN: PYROXENES